Prospecting New Antimicrobial Peptide from *Gracilaria* spp. Active-peptide Hydrolysate against Pathogenic Bacteria using Proteomic Approach

Klara Kharisma Bunga Chandra[1], Tri Rini Nuringtyas[2], and Tri Joko Raharjo[1,*]

OPEN ACCESS

[1] Biotechnology, Faculty of Graduate School, Universitas Gadjah Mada, Indonesia
[2] Faculty of Biology, Universitas Gadjah Mada, Indonesia
[3] Department of Chemistry, Faculty of Mathematics and Natural Sciences, Indonesia
*Corresponding Author:
trijr_mipa@ugm.ac.id

Received: 25 April 2024
Accepted: 12 December 2024
Published: 30 December 2024
Academic Editor: Dr. R. Haryo Setiarto, S.Si, M.Si

 Accreditation Number:148/M/KPT/2020. ISSN: 2089-5690, e-ISSN: 2406-9272. https://doi.org/ 10.15578/squalen.829

Abstract

Our study focused on unveiling the tropical red algae *Gracilaria* spp. Active-peptide materials from the central region of Java Island, Indonesia. We described the protein isolation, hydrolysis, purification, and method to test its potency against pathogen *Staphylococcus aureus* IFO 12576 and *Eschericia coli* IFO 3301, followed by molecular docking analysis. TCA/acetone precipitation was used to isolate *Gracilaria* spp. proteins, and the hydrolysis was done by trypsin digestion with an effective yield to provide antibacterial activity. The disk diffusion method showed promising inhibition and continued with a confirmation test using microdilution, which implied bacteriostatic inhibition with a minimum concentration of 40 µg/ml, from one potent fraction. Further characterizations were conducted using a proteomic approach. LC-HRMS was used for peptide sequencing in the potent fraction with prospective peptides identified along with its physical properties. Molecular docking simulations were used to investigate the degree of interactions using binding affinities score (kcal/mol), with the target of receptor DraE adhesin subunit (2JKJ) of *Escherichia coli* binds chloramphenicol. We proposed the interactions model of peptides GP1 and GP4 against targeted peptides. Our model GP4.1 and GP4.2 model (VVINADAK) were found to have high binding affinities with the energy score of -10,6 and -10,8 kcal/mol, respectively by the different sites of binding than chloramphenicol succinate.

Keywords: LC-HRMS, peptides, antimicrobial peptide, *Gracilaria*, hydrolysate

Introduction

Antimicrobial resistance (AMR), described as changes in the bacteria (phenotypic or genomic) causes the drugs (antibiotics) that are used to treat the infection to become less effective, nowadays raising attention since the threat obstructs various aspects ofhuman living. The Centres for Disease Control and Prevention shows data on 6 pathogenic bacteria species with the highest expression of resistance genes, namely *Escherichia coli*, *Staphylococcus aureus, Klebsiella pneumoniae, Streptococcus pneumoniae, Acinetobacter baumannii*, and *Pseudomonas aeruginosa*, with 3.57 million deaths due to AMR in 2014 and probably increase within years of antibiotics exposure. An example of resistance cases related to chloramphenicol resistance, with conventional bacteriostatic activity is known as 50s ribosome complex binding. These familiar binding sites raise evolution ability which induces a detoxification stimulant. The mechanism of chloramphenicol resistance generally occurs in the CAT1 complex caused by the chloramphenicol acetyltransferase (CAT) enzyme (Yu *et al.*, 2021), which catalyzes the transfer of the acetyl group from acetyl-coenzyme A (AcCoA) to the 3-hydroxyl CAM group (Biswas *et al.*, 2012) and detoxify chloramphenicol's active sites. This occurrence forces the necessity for other compounds that can restrain bacterial growth with different inhibition mechanisms, such as antimicrobial peptides.

Antimicrobial peptides (AMPs) are compounds owned by organisms that function as the body's defence system consists of less than 20 peptides (Cotton *et al.*, 2019). In this study, we focused on AMPs definition as small peptides with active site ability for antibiotics. These low size peptides can be obtained by isolating targeted peptides or cutting high molecular

mass protein into its smaller derivatives (Beaulieu *et al*., 2015; Sun *et al*., 2022). In Particular , this cutting was done using protease hydrolysis such as trypsin. Trypsin digestion for protein commonly occurs naturally as gastrointestinal enzymes which implies the plausible AMPs creation in the gut. AMPs attack the outer membrane thereby disrupting the conformation of the cell wall and the bacteria lose their body pressure balance (Bahar & Ren, 2013;Gogoladze *et al*., 2014;Huan *et al*., 2020). Some studies mentioned about the membrane integration of AMPs, which completely differentiates the commercial drugs from their attacking mechanism (Ciumac *et al*., 2019; Lei *et al*., 2019; Li *et al*., 2021). However, the complete and comprehended description of the AMPs targeted mechanism remains to be performed.

According to a previous study, various potential AMPs were isolated from marine algae which commonly perform host defensive mechanisms (Garcia-vaquero *et al*., 2019; Sun *et al*., 2022). Peptide compounds explored from algae are thought to provide active sites that can be proposed for active inhibitors. Red algae (Rhodophyta) have higher levels of peptides than the Phaeophyta and Chlorophyta groups (Conde *et al*., 2013). Apart from the polysaccharide characteristics, red algae species provide unique properties of the pigment-protein with notable identified structures (Chuang *et al*., 2023; Kawasaki *et al*., 2020; Pajot *et al*., 2022). Furthermore, several algae species exhibit a strict ecological relationship with a pathogen and produce AMPs as its secondary metabolite context might be particularly suitable for the use as sustainable biological controlling agents for pests and pathogens (Alvarez *et al*., 2023; Barre *et al*., 2022; Hwang *et al*., 2020; Maliki *et al*., 2022; Naik & Kumar, 2022).

Antimicrobial activities of seaweed extracts, which displayed an action against several *Gram*-positive and *Gram*-negative bacteria, have been previously reported in several studies(Beaulieu *et al*., 2015; Chiara *et al*., 2021; Mishra, 2018; Naik & Kumar, 2022; Teixeira *et al*., 2007). For instance, lectins isolated from the red algae *Eucheuma serra* and *Galaxaura marginata* strongly inhibit *Vibrio vulnificus* (Liao *et al*., 2011). Another research also showed that lectin inhibitor compounds from *Solieria filiformis* could inhibit the growth of *Gram*-negative and *Gram*-positive pathogenic bacteria at a concentration of 1000 µg/mL (Holanda *et al*., 2005). Peptide-bonded carbohydrate compounds from the red algae B. *triquetrum* and B. *seaforthii* have been shown to hinder the adhesion of *Streptococci* to the pellicle layer of tooth enamel, thereby preventing the main stage of dental plaque formation. Lectins from B. *seaforthii* inhibit the growth of *Streptococcus sanguis*, *Streptococcus mitis*, *Streptococcus sobrinus* and *Streptococcus mutans* by 75% (Teixeira *et al*., 2007). Those background of study leads to our interest in finding potential sources. We use *Gracilaria* spp. as it has a high protein content, with lower complex polysaccharides compared to other cultivated red algae. Despite the abundant source of protein and peptide model of *Gracilaria*, the peptide hydrolysates have not yet been defined for their antibacterial activity against neither *Gram*-positive nor *Gram*-negative bacteria. Therefore, this study reported our findings in peptide hydrolysate of *Gracilaria* spp. from Java Island, Indonesia as an antibacterial against Escherichia coli and Staphylococcus aureus. We used in vitro digestions for isolated proteins, focusing on peptide characterizations (LC-HRMS standard protocol) and its bioactivity test. This study determines molecular mechanisms of AMP by attacking active sites of the DraE adhesin subunit of *E. coli* in comparison with the native ligand chloramphenicol (CLM) that has been known for its resistance mechanisms. This preliminary proteomic study for *Gracilaria* spp. proposed the potency of peptide inhibition toward the growth resilience of pathogenic bacteria using its small peptide with a low molecular weight.

Material and Methods

Materials

Acetone analytical grade Sigma-Aldrich, sterile distilled water, liquid nitrogen, aquabidest, 0.05 M ammonium bicarbonate (Sigma-Aldrich®, USA), 1 mM hydrochloric acid (HCl) (Merck, Germany), methanol (Merck, Germany). The precipitating agent is ammonium bicarbonate, TCA 15-50% (Sigma-Aldrich, USA) ACS reagent T6399, acetone analytical grade (Sigma-Aldrich, USA). The ingredients for the fractionation were *Gracilaria* spp. peptide, methanol analytical grade (Merck, Germany), Amicon ultra–15 Centrifugal Filter Devices MWCO 3000 Da, trypsin sequence grade (Merck) enzyme. Materials for the antibacterial test are peptide hydrolysate samples with a certain concentration, Phosphate Buffer Saline (PBS), Luria-Bertani bacterial culture media (Himedia cloning media), Mueller-Hinton Broth (Sigma-Aldrich for Bacteriological culture), *Eschericia coli* IFO 3301 bacterial culture, *Staphylococcus aureus* IFO 13276.

Instrumentation

The tool used in this study was the *Gracilaria* spp. extraction tool. Namely blender, semi-analytical balance, 500 mL beaker, 150 mL and 300 mL porcelain cup, maceration cupboard and oven. The equipment used in the hydrolysis and fractionation of peptides are laboratory glassware, UV-Vis spectrophotometer (Shimadzu UV-1800), digital scales (Denver AA-250),

column HyperSep Retain PEP Cartridge 1 mL (Thermo Scientific), Amicon® µltra –15 Centrifugal Filter Devices 3 kDa MWCO (Sigma-Aldrich®), vortex mixer (Thermo Scientific, USA), centrifuge Sorvall Biofuge Primo R (Thermo Scientific, USA), incubator (EM-200T Sakura, Japan), autoclave, aerator, bulb, vessel, conical tube. Other tools for activity testing and analysis of peptide fractions are 96-well plates (Biorad), High Resolution Mass Spectrometry (Thermo Scientific Q Exactive Hybrid Quadrupole-Orbitrap Mass Spectrometer), Discovery studio software, protein model visualization with Chimera 1.3, Haddock 4.0 and Proteome Discoverer Ver software 2.5 (Thermo Scientific, USA).

Preparation and Extraction of *Gracilaria* spp.

Sample preparation and *Gracilaria* spp. extraction following the previous method (Beaulieu *et al*., 2015). *Gracilaria* spp. samples were obtained from Balai Besar Perikanan Budidaya Air Payau (BBPBAP), Jepara, Central Java, Indonesia. After cleaning, samples were freeze-dried at -40ºC. About 500 mL of phosphate buffer (pH 7) was added to 30 grams of crushed dry sample at room temperature for precipitation.

Protein precipitation with TCA Acetone

Acetone TCA has been done based on Niu et al. (2018) with some modifications. In 2.0 ml of extraction solution containing sterilized aquadest, the refined algae samples were homogenized and sonicated. The homogenate was placed in an Eppendorf tube and centrifuged for 5 minutes at 15,000 g. Cold 15% TCA/ acetone (1:1, v/v, with 15% TCA/50% acetone) was added to the protein extract, placed on ice for 5 min, centrifuged at 6500 g for 3 min, and the supernatant was discarded. Next, the protein precipitate was washed with 80% acetone and centrifuged. Finally, the protein precipitate was air-dried for 1–3 min and dissolved in ammonium bicarbonate for protein analysis.

Algal Protein Hydrolysis

The first-step protein extract was hydrolyzed with trypsin. Protein was dissolved in pH 7 ammonium bicarbonate (Raharjo et al., 2021). Trypsin was added to the dissolved protein at various enzyme and substrate ratios of 1/20, 1/25, 1/30, and 1/35 (w/w) and hydrolyzed at 30 °C for 24 h with constant agitation. An oven at 90 °C for 10 minutes stopped the enzyme after incubation. The 3 MWCO (Molecular Weight Cut-Off) amicon ultrafiltration-filtered hydrolysate was centrifuged at 3,000 g for 1 minute at 4°C, and the supernatant was protein hydrolysate. The Hydrolysis rate is expressed as percent absorbance before and after enzymatic hydrolysis. BCA (Bicinchoninic Acid) reagent at 562 nm was used to detect hydrolyzed peptide concentrations.

The degree of hydrolysis can be calculated by the following formula:

H = (Peptide absorbance (>3 kDa)) / (total peptide absorbance of the sample) x 100%

Cationic exchange (SCX) and HyperSep Retain PEP salt removal continued protein purification. The protein hydrolysate fractionated in citrate and phosphate buffer gradient pH 3; 4; 5; 6; 7; 8 and 9. Peptide fraction was purified by SPE with a polar enhance polymer (PEP) cartridge and methanol as an eluent.

Antibacterial test

Disc diffusion

Escherichia coli IFO 3301 and *Staphylococcus aureus* IFO 13276 isolates were obtained from The Center for Food and Nutrition Studies at Gadjah Mada University and were tested for antibacterial activity. Firstly, in the pre-culture stage, bacteria were incubated at 37ºC in MHB. Then, an MHA plate was used for antibacterial investigations. Next, indicator bacteria inoculum (OD 600 0.1) was spread evenly with a sterile cotton swab in an MHA petri dish in the first stage. The blank Oxoid disc was put into the MHA plate agar for antibacterial susceptibility. 4 discs were used as treatment, there are 250 µg/ml chloramphenicol (CLM) as the positive control, the negative control as a sterile liquid medium, and duplicate sample peptides dissolved in sterile sterilized distilled water (SDW). Results from the inhibition zone on the disc diffusion method:

Inhibition zone=clear zone diameter-disc diameter.

Microdilution

For pre-culture, the bacteria were incubated at 37ºC in MHB (5 mL) for 24 hours and the indicator bacterial inoculum (OD 600 0.1) was cultured in reaction tubes. Next, the OD adjustment was done by UV spectrophotometers at 600 nm 0.5-0.7 (both bacteria). Microplate-96 was prepared, media was added to each well (up to 200 µL), peptide fractions (1µg/mL) were added (20, 30, 40, 60, 80, 100, 200 µL), and 50 ìL of bacterial culture was added to each well. About 10 ìL of liquid mixture was poured for initial dilution on the well filled with liquid media (100 µL) and diluted (10 µL) into the next well (100 µL) until it reached $1x10^{-5}$ ìL. The samples were incubated at 37ºC for 20 hours. The absorbance was measured and the calculation for MIC was addressed. The percent inhibition of the peptide fraction against bacterial samples was the

decrease in OD from the negative control (without the peptide fraction). Percent inhibition calculation:

% Inhibition= (OD control negative (blank)-OD fraction test)/(OD control negative (blank)) x 100%.

Peptide characterization using LC-HRMS

The peptide fraction of the protein hydrolysate that is most active as an antibacterial is then determined by the amino acids that make up the peptide through mass analysis with High Resolution Mass Spectrometry (HRMS). A total of 5 µL of sample (sampler temperature maintained at 5°C) of hydrolysate was injected onto an Acclaim® PepMap RSLC column (C18, 75 µm × 150 cm, with a particle size of 2 µm and a pore size of 100 Å). The peptides contained in the column were eluted using two mobile phases, namely mobile phase A (water and 0.05% formic acid) and mobile phase B (water: acetonitrile 20:80 and TFA 0.1%). Mobile phases A and B then used a certain gradient with a flow rate of 0.3 µL/minute. MS and MS/MS were carried out using the NSI ionization method. Nitrogen is used as sheath and auxiliary gases and is set at 10 and 5 units. The NSI probe was set at 4000 V, and the ion transfer tube at 300°C. MS detection uses positive ion mode which operates in high resolution and accurate mass mode. For MS/MS analysis of peptides, the m/z range 350-1800 was used using full MS dd-MS2 mode. The full-MS parameters were resolving power set at 140,000 (FWHM) using automatic gain control target at 3×106 and maximum ion injection time at 100 ms. Meanwhile, the dd-MS2 parameters used are resolution set at 17,500 (FWHM), automatic gain control target at 1×105, maximum ion injection time at 105 ms, loop count / topN 20, isolation window 1.2 m/z, and collision energy at 27. Analysis by MS was carried out for 90 minutes. Chromatograms were obtained from Xcalibur by Thermo Scientific software.

Molecular prediction method

The 3D secondary structures of potential peptides were built using PEP-FOLD v4 web server (https://bioserv.rpbs.univ-paris-diderot.fr/services/PEP-FOLD/). The Master protein structure was downloaded from RSCB Protein Data Bank (https://www.rcsb.org/) for ligand CLM and 2JKJ DraE adhesin. Protein structure was visualized using Discovery Studio 2021 and Chimera 1.3. Molecular docking analysis was performed by High Ambiguity Driven protein-protein Docking (Haddock v.2.4) (Honorato *et al.*, 2021).

Results and Discussions

In this section, we discussed data investigated in protein hydrolysate of *Gracilaria* spp. for its antibacterial activity. The coverage of hydrolysate detections implies that small molecules were obtained using the established procedures.

Protein extraction results

The acetone and trichloroacetic acid (TCA) combination treatment for extraction was conducted (Table 1). To reach a high yield of proteins, both methods (TCA 15%+acetone and acetone 100%) are used. TCA was added at 15% and the yield was compared to the acetone only treatments as pre-treatment (Niu *et al.*, 2018). The two methods differ in protein texture and color. The addition of TCA creates a hydrophobic structure that is insoluble in acetone and water. From this experiment, 35,35 mg protein was the highest yield extracted using acetone only, while the addition of TCA only reached a maximum yield of 29,68 mg protein from a dry weight 4 grams. Previous work on protein precipitation using PBS and TCA showed the purified protein *Gracilaria acerosa* 31.07% and *Halimeda macroloba* at about 28.94%, *Halimeda tuna* 23.12% and *Cladophora glomerata* (20.38 ± 0.73%) from the total dry weight (Boob *et al.*, 2010). Crude protein extracts from *Gracilaria edulis* were 1.9 mg/mL in aqueous and 2.7 mg/mL in methanol extract respectively. TCA/acetone precipitation is thought to minimize protein degradation and activity of proteases as well as reduce contaminants such as salts or polyphenols (Niu *et al.*, 2018) contradicting our findings which implemented only acetone provided a more promising yield. Hence, according to the highest yield, this study used acetone precipitation for further experiments.

Hydrolysis Results

Protein hydrolysates are defined as smaller fragments of protein, essentially produced by enzymatic hydrolysis of whole protein sources by appropriate proteolytic enzymes under controlled conditions, followed by post-hydrolysis processing to isolate desired and potent bioactive peptides from a complex mixture of active and inactive peptides (Nasri, 2017). In this study, we performed hydrolysis techniques by using trypsin as one of the most abundant sources of protease, and its existence in living organisms. Trypsin has active groups of serine, histidine, and asparagine which cleavage the lysin and arginine residues (Olsen *et al.*, 2004). Moreover, using trypsin also efficiently managed the preparation for further analysis using mass spectrometry. Since

antibacterial peptides isolated from natural sources commonly consist of 12-50 residues, the hydrolysates from trypsin were filtered using a 3 kDa filter to obtain small active peptides (Hancock & Sahl 2006). We are concerned with performing the test by using <3kDa, to enlarge the objective view of the inhibitions strategy for high spectrums of antibiotics. Despite the structures and active site, the size of molecules is an important aspects of targeting the inhibition growth of bacteria (Alanis, 2005; Kowalska-Krochmal & Dudek-Wicher, 2021).

Based on BCA reagent absorbance test data, enzyme hydrolysis at 1:30 yields maximum cutting with 91% hydrolysis (Table 2, Fig. 1). This result proved that reducing enzyme use in digestion process will not interfere with enzyme hydrolysis. However, this research continuously uses the ratio 1:30 for the digestion process in terms of efficiency. Incubation time is also optimized by varying the time, resulting in a consistent increase in the degree of hydrolysis (DH) up to 20 hours, followed by a decrease in 24 hours of incubation (Fig. 2). This result was then used to generate a new antibacterial peptide from macroalgae *Gracilaria* spp. protein hydrolysate.

Arginine and lysine carboxyl residues are produced by trypsin cutting (Tu *et al*., 2017). Ionic precursors with double charges are easily fragmented when trypsin cleaves peptides (Steen & Mann, 2004). At 37°C and 7.5-8.5 pH, trypsin hydrolysis is optimal. The Previous study mentioned that the highest yield of *Ricinnus*

Table 1. Crude protein absorbance and concentration

Sample ID[1)]	595nm (Abs)	mg protein	NH_4HCO_3(ml)	mg/ml
grctca	0.075	11.68	5	2.34
grctca	0.183	29.68	5	5.94
grctca	0.116	18.52	5	3.70
grcact	0.217	35.35	5	7.07
grcact	0.102	16.18	5	3.24
grcact	0.130	20.85	5	4.17

[1)]grctca, extraction of *Gracilaria* protein with 15% TCA; grcact, pure acetone.

Table 2. Trypsin hydrolysis results at various ratio

protein (µg/µl)	enzymes (µg/µl)	hydrolyzed (µg/ml)	Unfiltered (µg/ml)	% hydrolysis
2	400	344.28	364.29	0.82
2	500	337.14	833.43	0.59
2	600	311.86	176.43	0.91
2	700	309	320	0.84

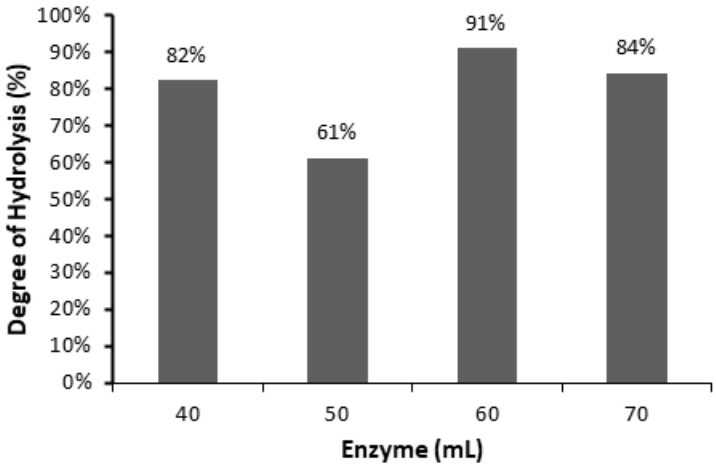

Figure 1: The degree of hydrolysis from protein extract in different ratios (enzyme:protein).

comunis 9.14% of the total peptides present in the hydrolysate was obtained from the pH 4 fraction, whereas the lowest yield was obtained from the pH 8 fraction (Raharjo *et al*., 2021) which was slightly different from our samples. Next, based on its fractionation, the molecular cut off 3000 Da selected only the small peptides that are plausible to explain the significant reducing yield (Fig. 2).

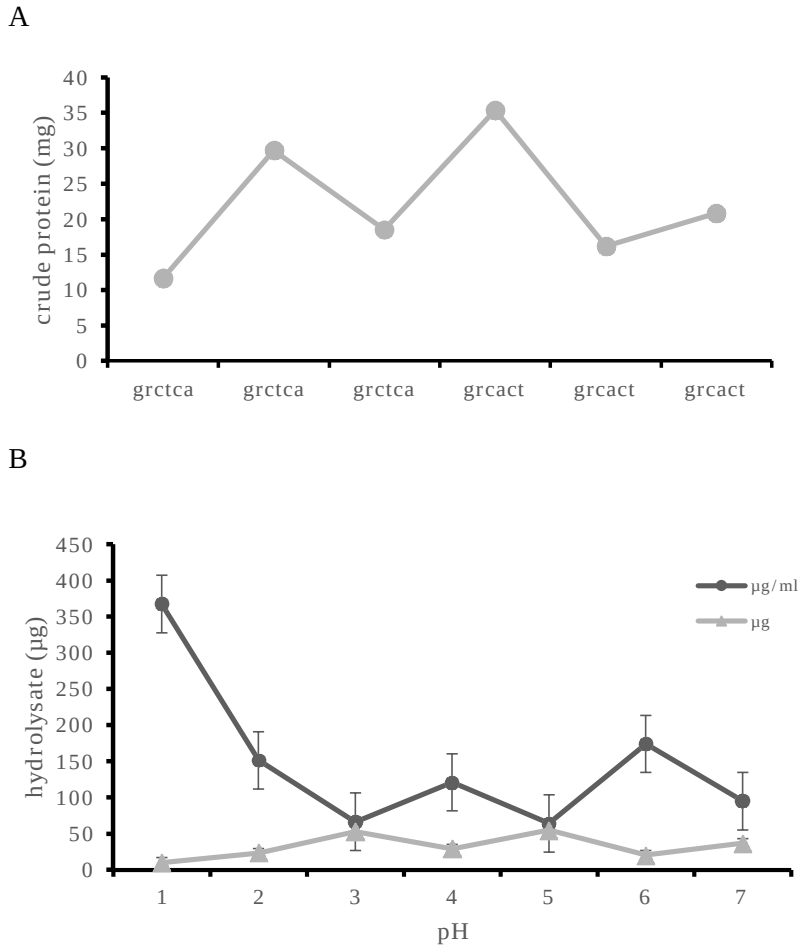

Figure 2: The yield of A) protein (mg) extracted using different methods (grctca, tca 15%; grcact, acetone) and B) its hydrolysate samples (ìg) using trypsin in the 1:30 enzyme per protein ratio, which was fractioned using SCX cationic exchange.

Antibacterial activity results

BCA reagent absorbance measurements of the peptide fraction are shown in Table 3 for concentration preparation before antibacterial assay which is then adjusted into sample concentration 350 ppm. Those data showed the different concentrations of peptide fraction by using various ranges of pH, since peptide has the optimized pI score, and we aim to screen the interactive active sites against bacteria. Here, we found the high concentration of peptide accumulated in pH 3 (Table 3).

Table 3. Absorbance and concentration of peptides with BCA reagent

pH	absorbance	Concentration (µg/ml)
3	0.279	367.4
4	0.181	151.3
5	0.156	66.3
6	0.173	121
7	0.156	64
8	0.189	174
9	0.165	95

The result of the activity test with the disc diffusion method is shown in Table 4. Both bacteria showed active activity at pH 3 with significant inhibition using the disc diffusion method. The following table shows the inhibition zone's sample diameter. The activity screening showed pH 3 was the only active fraction with a slight clear zone as compared to the chloramphenicol (Fig. 3). As shown in the picture, the peptide actively inhibits the growth of either *Gram*-positive or *Gram*-negative bacteria. However, the peptide structure and condition have not been analysed in the real time condition. Cationic peptides were eluted in most of the lowest pH range, consistently. It can be proposed that the inhibition of peptides in the low pH was basically due to the cationic charge, but the assumption should be followed by molecular dynamics interactions between membrane and peptides integration. This study showed a similar result to Beauliu *et al.* (2015) which reported antibacterial activity The >10 kDa protein trypsin hydrolysate fraction exhibited activity against the bacterium *Staphylococcus aureus* with a significant decrease of the maximum specific growth rate from concentrations of 0.31 mg/mL to 2.5 mg/mL.

Table 4. The peptide concentration test and diameter of inhibition zone in the antibacterial test using disc diffusion method

pH fraction	Mass (µg)	Volume (µl)	Inhibition zone diameter (mm) of S. *aureus*	Diameter of inhibition zone (mm) E. *coli*
3	3.67	20	1.33±0.39	1.97±0.12
4	3.78	25	-	-
5	3.32	50	-	-
6	3.63	30	-	-
7	3.52	55	-	-
8	3.48	20	-	-
9	3.80	40	-	-
CLM	0.50	20	7±1.61	9.5±0.05

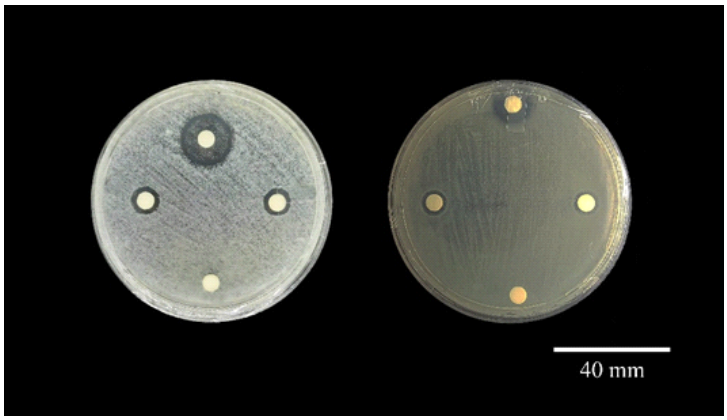

Figure 3. The disc diffusion clear zone from A) S. *aureus* IFO 13276 and B) E. *coli* IFO 3301; both using pH 3 dissolved peptide with the visible clear zone. CLM referring to positive control chloramphenicol

Antibacterial test using the disc diffusion method

For further validation of peptide activity, the microdilution method was used (Fig. 4). It is confirmed that the peptides diluted in pH 3 showed activity inhibition of over 50% in both bacteria. The inhibition value of *S. aureus* bacteria was 37% at 30 minutes of incubation and reached 86% after 24 hours. The inhibition value for *E. coli* bacteria did not occur at 30 minutes of incubation, growth reached nearly double absorbance, but after 24 hours of incubation, there was an inhibition of up to 50%. This phenomenon suggests that the growth inhibition mechanism from active peptides takes time to work effectively as is shown in the growth curve (Figure 4). Then at 24 hours of incubation, the bacteria grew to OD 0.194 and 0.212. In S. *aureus* bacteria, 30 minutes of incubation gave OD growth of 0.24 and 0.13 after 24 hours of incubation to OD of 0.23 and 0.197. Although

the absorbance increased, the growth of both bacteria was much lower compared to the negative control whose growth increased by 100% to full growth with OD values ranging from 0.3 to 0.8. The data implied that the microdilution may have bacteriostatic type of inhibition (Fig. 4). This approach performed higher concentration than other extracts derived from organic solvent, such as R. *mesenterica* ethanol extracts was observed, with MIC values in the range 0.06 to 32.00 ìg/ml against tested strains (Skoèibušiæ *et al*., 2019), S. *obliquus* hexane: chloroform extract in the range 15.6–125 µg/mL (Mukherjee *et al*., 2022), *Rhodophyta* showed antibiofilm activity against E. *coli* with $MBIC_{50}$ and $MBIC_{90}$ values of 64 and 512 µg/mL (Alsenani *et al*., 2020).

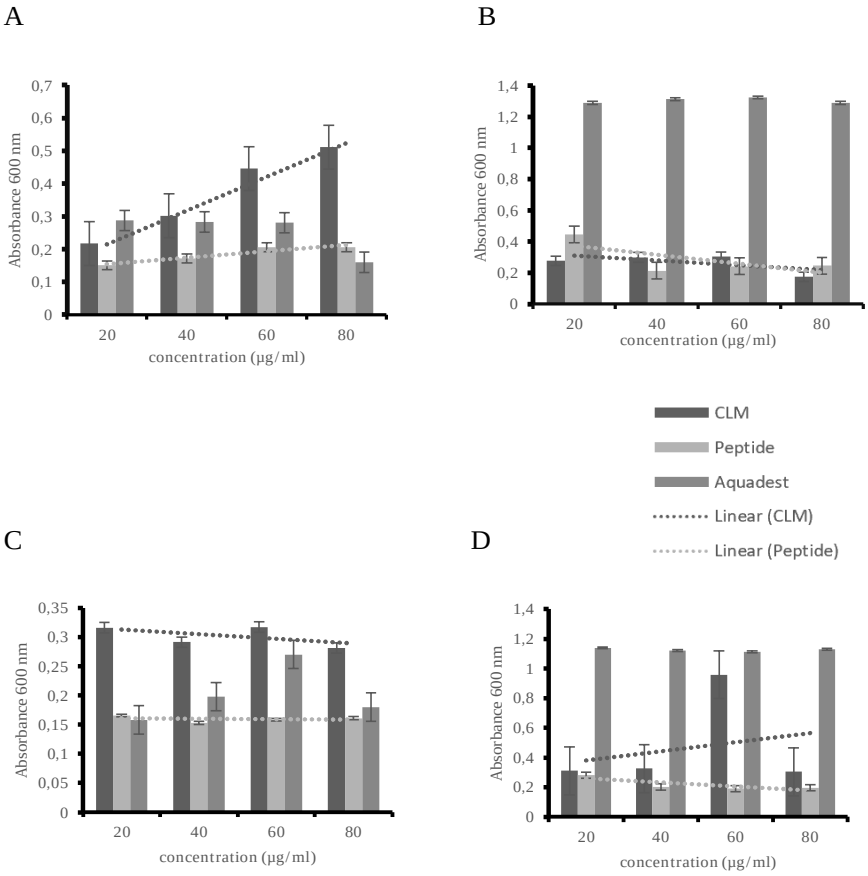

Figure 4. The growth of the targets bacteria during 30 minutes (A,C) and 24 h (B,D) of incubation. A-B showed the activity against E. *coli*; C-D showed the activity against S. *aureus.*

Peptide identification and characterization

Following the activity provided by peptides fraction, we aimed to further characterise our substances. Here, we provide an LC-HRMS analysis of active peptides, the result of which is shown in Table 5. We tentatively assumed that the bacteriostatic inhibition occurred during the incubation period in which the mechanism may depend on its structure.

Based on the data obtained, our sample *Gracilaria* sequenced the longest 13 amino acids with a mass of 1263.64 daltons and the shortest 8 amino acids with 829.447 daltons, and interestingly, the sequence has no longer than 20 AAs. Some peptides are identified as membrane composition proteins, which can be assumed as the pigment binding proteins. For example, Allophycocyanin reads dominated (Apc) in this study, there are SIVNADAEAR (Table 6) and EVTSSLVGTDAGK (Table 7), while the shortest sequence has having similarity with cytoplasmic polyadenylation element (Table 8). Phycocyanin as a pigment binding protein complex found in the thylakoid membrane as the outer layer of cyanobacteria, which may be found also in the higher generation of algae (Asayama, 2012). It is also confirmed that our peptides M2WWX8 and A0A1Z1M1P5 have similarities with other red algae species, while the other sequences remained unidentified. Therefore, these secondary structures are shown in the allophycocyanin complex from *Gracilaria chilensis* in both alpha and beta subunits

(Charlesworth *et al*., 2013). The SIVNADAEAR for Photosystem II complex cytochrome c-550 also found in other 145 red algae species, such as *Melanthalia intermedia, Gracilaria spinulosa, Gelidium elegans, Gracilariopsis chorda, Gracilaria ferox, Agarophyton chilensis, Agarophyton vermiculophyllum, Crassa caudata, Hydropuntia rangiferina, Gracilaria changii, Gastroclonium compressum, Gracilaria edulis, heteroclada, mclachlanii, Crassa firm*a. These findings proved that the purification retrieved the conserved region of *Gracilaria*. However, the complete sequence of this *Gracilaria* spp. used in this study remained unknown.

Table 5. LC-HRMS peptides sequences from *Gracilaria* spp. Hydrolysate and its physical properties

Protein ID	Sequences	[MH+] Da	pI	Coverage	Net charge	Function
GP1	VVINADAK	829.47779	5.31	8%	0	Cpe B Gracilaria changii
GP2	TVTLEESGK	963.49932	5.54	4%	-1	Cytochrome c-550
GP3	SIVNADAEAR	1045.52726	5.60	5%	-1	Allophycocyanin alpha subunit
GP4	EVTSSLVGTDAGK	1263.64269	4.89	4%	0	Allophycocyanin beta subunit
GP5	SHNGSDEWK	1059.44901	4.55	6%	-1	Selenium-binding protein
GP6	SAAEQSAPE	889.38977	7.37	5%	-2	MBL fold metallo-hydrolase
GP7	GAEDGNVYDEK	1196.50659	6.07	2%	-3	Uncharacterised protein Porphyra umbilicalis
GP8	DVVDAImGLTmN	1310.59667	4.55	6%	-1	Nascent polypeptide Gracilariopsis chorda (modified)

Table 6. The SIVNADAEAR (GP3) y+ and b+ peak of LC-HRMS spectra

#1	b^+	b^{2+}	Seq.	y^+	y^{2+}	#2
1	88.0393	44.52329	S			10
2	201.1234	101.0653	I	958.4952	479.7513	9
3	300.1918	150.5995	V	845.4112	423.2092	8
4	414.2347	207.621	N	746.3428	373.675	7
5	485.2718	243.1396	A	632.2998	316.6536	6
6	600.2988	300.653	D	561.2627	281.135	5
7	671.3359	336.1716	A	446.2358	223.6215	4
8	800.3785	400.6929	E	375.1987	188.103	3
9	871.4156	436.2114	A	246.1561	123.5817	2
10			R	175.119	88.06311	1

Prediction of the probability value shows the tendency of the secondary structure when visualizing the 3D model using Pep-fold 3. Nearly all the sequences detected from LC-HRMS showed a low molecular mass, less than 1000 Da. As compared to a previous study, the SDS-PAGE of purified phycocyanin reconfirmed the presence of single bands of the á-subunit 18.4 kDa and â-subunit 21.3 kDa (Aoki *et al*., 2021). The study mentioned three cylinder scores of phycobilisomes, which are compatible with the presence of a 90 kDa linker core (Jose *et al*., 2017). The secondary structure of helical or á-helix peptides is characterized by hydrogen bonding in the -CO (i-th residue) and NH (i+4)th residue groups, resulting in high hydrophobicity (Fig 5). The â-Sheet structure is shown by the presence of hydrogen bonds from the N-terminal, both parallel and opposite. If they are parallel, they are called parallel, while opposites are called antiparallel. The coil or random coil model is formed from random or irregular hydrogen bonds. The formation of loops in the secondary structure of the á-helix and â-sheet is caused by the polar amino acid

residues alanine, glycine, serine and tyrosine (Iolovitch, 2020). The formation of the loop results in a decrease in hydrogen bonds, so it is hydrophobic (Wang et al., 2016). Glycine is a polar amino acid and tends to form permanent loop patterns. Meanwhile, proline has the opposite property, namely hydrophilic. In our peptide, EVTSSLVGTDAGK (GP 4) as the longest peptides showed numbers of glycine amino acid residue. The glycine was predicted to form a hydrophobic chain that possesses higher binding with the targeted hydrophobic membrane.

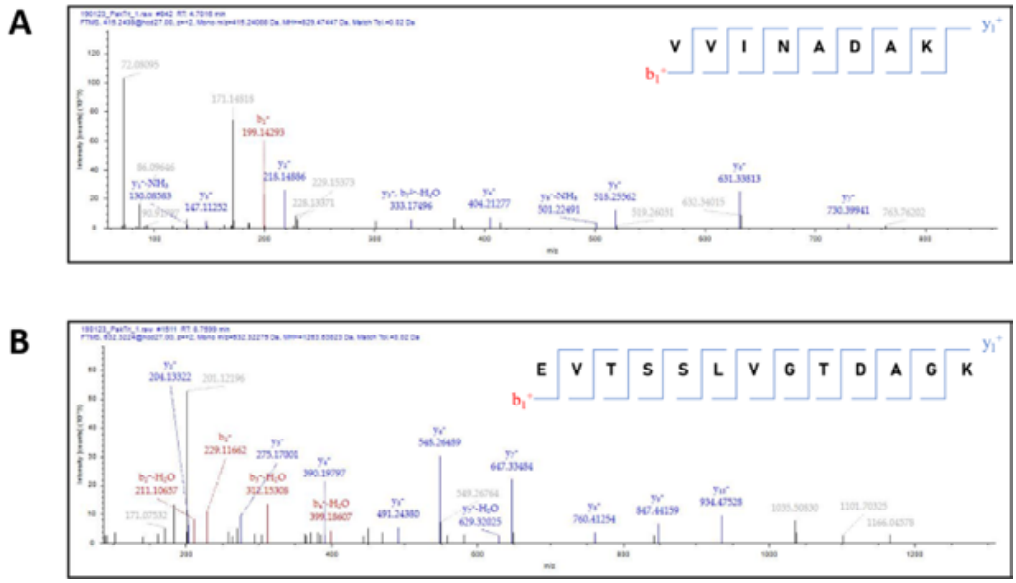

Figure 5: LC-HRMS Spectra of A) GP1 and B) GP4 for further molecular docking analysis.

Table 7. The EVTSSLVGTDAGK (GP4) y+ and b+ peak of LC-HRMS spectra

#1	b^+	b^{2+}	Seq.	y^+	y^{2+}	#2
1	130.04987	65.52857	E			13
2	229.11828	115.06278	V	1134.60009	567.80369	12
3	330.16596	165.58662	T	1035.53168	518.26948	11
4	417.19799	209.10263	S	934.48400	467.74564	10
5	504.23002	252.61865	S	847.45197	424.22962	9
6	617.31408	309.16068	L	760.41994	380.71361	8
7	716.38250	358.69489	V	647.33588	324.17158	7
8	773.40396	387.20562	G	548.26747	274.63737	6
9	874.45164	437.72946	T	491.24600	246.12664	5
10	989.47858	495.24293	D	390.19832	195.60280	4
11	1060.51570	530.76149	A	275.17138	138.08933	3
12	1117.53716	559.27222	G	204.13427	102.57077	2
13			K	147.11280	74.06004	1

The spectra showed in the SIVNADEAR sequence, the m/z values for each amino acid are obtained, shown in Table 6. Each MS scan results in a mass spectrum in which subtraction scores of ionization residues (m/z) account for the detected peptides, with y+ and b+ referring to the direction of ionization. The detailed determination of peptide sequence is explained in this section. As for SIVNADEAR, it shows the sequences serine, isoleucine, valine, asparagine, aspartic acids, aspartate, alanine, and arginine. First, ionization on the b section showed a residue of ionization b1+ (88.06) belonging to serine. Continuously, the next ionization score shows the cutting residue of mono isotopic mass from whole peptides, starting from the higher score to the lowest score. The number indicated continuous ionization, resulting in a decreasing score until it reached the end of the sequence. The difference between the mass of y9+ (958.49523) and y8+ (845.41117) shows a value of 113.08406 monoisotopic mass of Isoleucine, then y8+ (845.41117) and y7+ (746.34276) shows a value of 99.06841 monoisotopic mass of Valine. Next, y7+ (746.34276) and y6+

(632.29983) show a value of 114.04293 as a monoisotopic mass of Asparagine, then y6+ (632.29983) and y5+ (561.26272) shows a value of 71.0371100000001 monoisotopic mass of aspartic acid. The difference between the mass of y5+ (561.26272) and y4+ (446.23577) shows a value of 115.02695 monoisotopic mass of aspartate. The difference between the mass of y3+ (375.19866) and y2+ (246.15607) shows a 71.03711 monoisotopic mass of Alanine. The difference between the mass of y2+ (246.15607) and y1+ (175.11895) shows a value of 175.11895 monoisotopic mass of Arginine (R), which marks the end of peptide sequences. The R cutting end of peptides also indicated that trypsin works effectively since trypsin specifically cuts the R and K amino acids.

Table 8. The VVINADAK (GP1) y+ and b+ peak of LC-HRMS spectra

#1	b^+	b^{2+}	Seq.	y^+	y^{2+}	#2
1	100.07569	50.54148	V			8
2	199.14410	100.07569	V	730.40938	365.70833	7
3	312.22817	156.61772	I	631.34097	316.17412	6
4	426.27110	213.63919	N	518.25690	259.63209	5
5	497.30821	249.15774	A	404.21397	202.61063	4
6	612.33515	306.67121	D	333.17686	167.09207	3
7	683.37227	342.18977	A	218.14992	109.57860	2
8			K	147.11280	74.06004	1

Table 9. The reading sequences from the master protein (RCSB) data bank

Sequences	Master Protein (RCSB)
α-subunit SIITK**SIVNADAEAR**YLSPGELDRIKSFVLSGQRRLRIAQILTDN RELIVKQGGQQLFQKRPDVVSPGGNAYGEEMTATCLRDLDYY LRLVTYGIVAGDVTPIEEIGLVGVKEMYNSLGTPISGVAEGVRS M KNVACSLLAGEDSAEAGFYFDYTLGAMQ β-subunit MQDAITSVINAADVQGRYLDDNSLDKLRGYFQTGELRVRASA TIAANAATIIKDSVAKALLYSDITRPGGNMYTTRRYAACIRDLD YYLRYATYGMLAGDPSILDERVLNGLKETYNSLGVPIGATIQA VQAMK**EVTSSLVGPDAGK**EMGVYFDYICSGLS	5TJF
MSIVTK**SIVN ADAEAR**YLSP GELDRIKSFV LSGQRRLRIA QILTDNRERI VKQAGQQLFQ QRPDIVSPGG NAYGEEMTAT CLRDLDYYLR LVTYGVVAGD	M2WWX8
PSILDERVLN GLKETYNSLG VPIGATIQAI QAMK**EVTSSL VGTDAGK**EMG LYFDYICSGL	A0A1Z1M1P5

In the EVTSSLVGTDAGK (Glu-Val-Thr-Ser-Ser-Leu-Val-Gly-Thr-Asp-Ala-Gly-Lys) sequence, the m/z values obtained for each amino acid are shown in Table 7. Intriguingly, this peptide has the longest sequences with a neutral charge (0) shown in Table 5. The structure of GP4 may be beneficial for its integration inside the bacteria cell membranes, hence attached directly as an inhibitor through molecular mechanisms.

The other interesting sequence is VVINADAK, showed the lower molecular weight among others. Accordingly, the physical properties seemed convincing to show the significant impact on the inhibitory mechanism by molecular mechanism as it has a neutral charge (0). VVINADAK is known to be a part of Cpe B or complex polyadenylation B from *Gracilaria changii*. Cpe B complex is the central factor that binds the CPEs and controls polyadenylation-induced

translation (Ivshina *et al*., 2014) which is plausible to bind into the bacterial protein regulations. Therefore, GP1 and GP4 (Fig. 5) were chosen as peptide candidates fort molecular docking analysis.

Peptide docking model

In this term, we aimed to know the inhibition mechanism of peptides, in comparison with chloramphenicol. Apart from membrane integration and cell-lysis targeted mechanisms, we use a molecular approach considering small peptide structure which allows these particles to freely integrated into the membrane and attacks enzymatic regulation such as hydrolase cell-walls (Cotton *et al*., 2019; Xiang *et al*., 2017), as it reflected on the bacteriostatic inhibitions. Furthermore, we use the DraE adhesin subunit of *Escherichia coli* as a representative of the chloramphenicol targeting model which uniquely discovered with potential intoxicated sites by bacteria. We suggest that the different target peptides of the attacking mechanism may confer multiple inhibition responses.

Docking is a method used to determine the interaction between a protein and a ligand or peptide on a particular active side. Computational docking is the prediction or modelling of the three-dimensional structure of biomolecular complexes, starting from the structure of individual molecules in free and unbound form (De Vries, Van Dijk & Bonvin, 2010). The mechanism of action was predicted with a 3D model of the substrate peptide according to the action of chloramphenicol on the test bacteria. Most AMPs reported to date can be characterized as one of the following four types based on their secondary structures: â-sheet, á-helix, extended, and loop (Ajesh & Sreejith, 2009; Huan *et al*., 2020; Li *et al*., 2021). Among these structural groups, á-helix and â-sheet structures are more common.

In this study, our findings determine that secondary structure peptides GP1 and GP4 showed both á-helix and â-sheet (Fig. 6). The structure between amino acids in this sequence does not appear to have any interactions that would allow a helical shape (Salwiczek *et al*., 2012), as there are no strong hydrophobic amino residues such as glycine, tyrosine, serine. In addition, the sequence does not contain any amino acids with benzene groups. In the docking model interaction, the ligand-receptor will be modelled and clustered based on its HADDOCK score (De Vries *et al*., 2010). The HADDOCK scoring function consists of a linear combination of various energies and buried surface area. Furthermore, we conducted an analysis of its energy-binding activity. We chose two best models for the representative peptides namely GP1 and GP4. It is based on the lowest energy score and the best haddock score for analysis, which are GP1.1, GP1.2, and GP4.1, GP4.2. The structure of the DraE and chloramphenicol (CLM) complex provides the starting point for the design of novel antimicrobial compounds. This modification evolved the structures for CLM-ligand complexes where the binding of CLM involves the burial of the benzene ring, the interactions seen in this model are focused on burial of the chlorines (Pettigrew *et al*., 2004). As our information, the summary was conducted by obtaining ligand interaction sites and the types of interactions. When it found the distinction between authentic ligand interaction sites, we concluded that our model could be accepted to have new prospects on bioactive material.

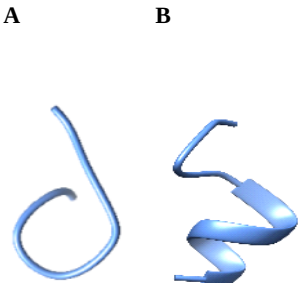

Figure 6. A) GP1-coil and B) GP4-â-sheet 3D structure by de novo PEP-FOLD v4 web server.

Chloramphenicol shows the inhibition of bacterial growth in adhesion complex DraE using hydrophobic interaction. TYR A:115 interaction shows the similarity between those ligands. The difference is that pi-alkyl interaction is shown in the chloramphenicol ligand interaction. Both the GP1 and GP4 peptides interact with chloramphenicol (CLM) ligands at residues PRO A:40, PRO A:43, and ILE A:41, but the two models interact differently. Both models share ILE A:144, GLY A:113, and TYR A:115 interactions. In GP4.2, the PRO A:40 alkyl binding interaction is a Van Der Waals force, in GP4.1, an alkyl interaction, and in CLM, a pi-alkyl

bond. The Van Der Waals forces at residues ILE A:144, GLY A:113, and ILE A:41 are common to all models (against the GP4.1). GP1.1 and GP1.2 have hydrogen bonds. Hydrogen bonds are strong, stable bonds in molecules. Pi-alkyl interactions at PRO A:43 were found in GP1.1, GP1.2, and GP4.2, but not in all peptide models. All peptide models have TYR A:115 alkyl interaction. GP4.1 shows an alkyl interaction between the LEU A:26 residue and Lysine's cationic group. The LEU A:30 residue attracts the GP4.2 and GP1.2 models.

Theoretically, the mechanism of action of antimicrobial peptides is categorized into two types, namely non-membrane approaches (enzyme, DNA, or RNA inhibition) and membrane integration (bacteriolysis) (Huan *et al*., 2020). The non-membrane approach occurs in types of peptides that tend to be coil-shaped and non-polar, so they can enter the cell wall and inhibit biomolecular pathways as it presents in the GP1 and GP4 (Fig. 6). At the present stage, the image of particles integration through membrane and cells imaging are expected to support the mechanism prediction for the specific bacteria. The result disclosed that respectively peptides GP1 and GP4 showed strong interaction with the DraE complex as compared to the chloramphenicol inhibition (Fig 7). Low energy forces the interaction to happe without other interfering agents in this model interaction. The finding indicated that peptides from active fractions may inhibit the growth of *E. coli* bacteria by intramolecular mechanisms more than cell wall degradations. In this stage, it remains unknown the peptide interaction and movement in the specific bond were created. However, the inhibitory effect assay of peptides from *Gracilaria* spp. using different mechanisms is needed for further investigation. Moreover, optimising peptide samples is important to manage the peptide conditions. This unique peptide purified from *Gracilaria spp.* is the first report to have antimicrobial inhibition activity. The development of a single active peptide must be followed by extensive techniques such as scanning electron microscope, molecular dynamics analysis, and other computational predictive components. This observation allows the design of novel therapeutics that maintain the geometry of the adhesin-CLM interaction. Moreover, the toxicity of nitro-benzene interactions against human ribosomes has yet to be determined.

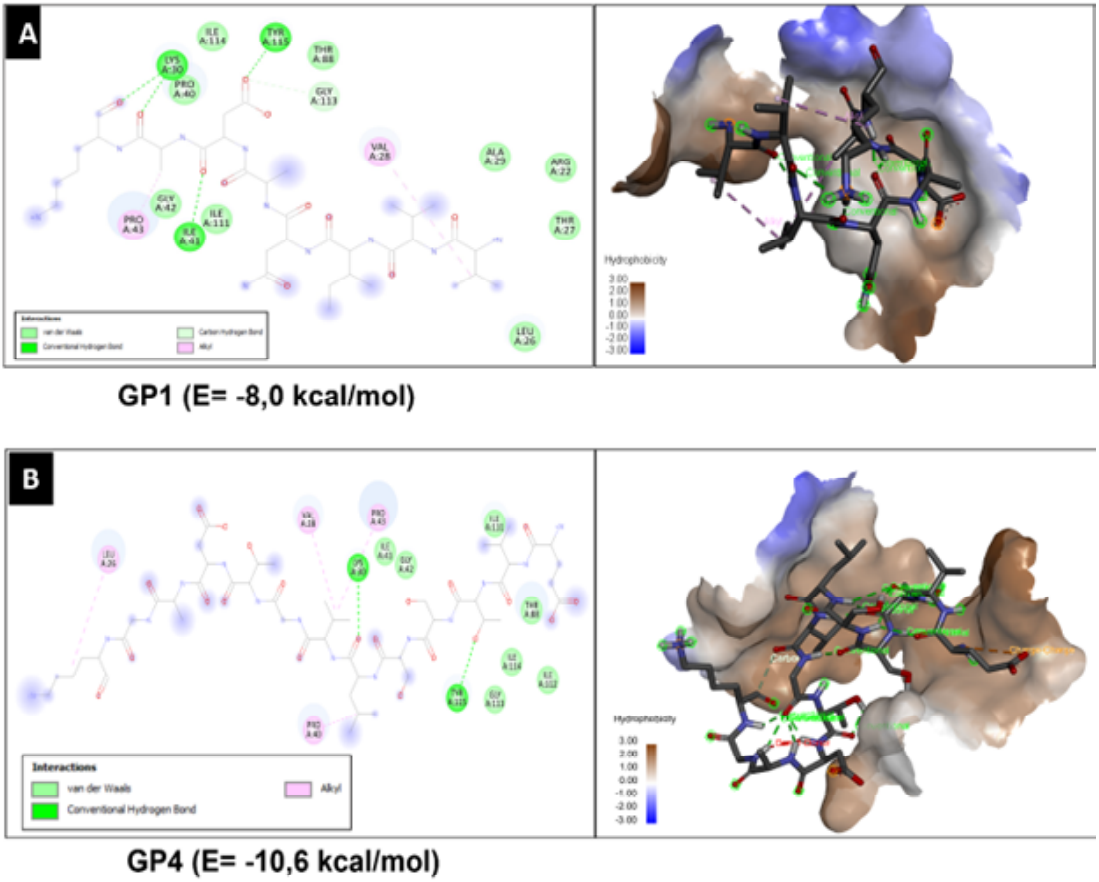

Figure 7. Interaction model between receptor DraE complex and the peptides A) GP1; B) GP4.

Conclusion

Our determination in inhibitory activity is considered lower than chloramphenicol but notated as clear inhibitions that can be improved in the future. Although there are thousands of AMPs in the database, the precise mechanism of their actions is barely known. At first, we promote the cationic site of peptides in which it develops inhibition activity towards receptors. Still, the peptide fractions charge and the growth pattern of bacteria seems to not match with the first hypothesis. Therefore, we suggest another plausible target mechanism such as a molecular mechanism or enzymatic promoter. In this case however, we have seen that compared to chloramphenicol, the inhibition sites were varied independently and totally distinct.

For future prospects, the determination of membrane integration by cationic sites of these peptides is necessary for future prospect. The conclusions from the research carried out that the protein hydrolysate from red seaweed *Gracilaria* spp. was successfully obtained by cutting the trypsin enzyme with an effective concentration (enzyme: substrate) of 1:30. The value of the degree of hydrolysis at a ratio of 1:30 is 91%. Antibacterial activity of the peptide fraction from hydrolyzed red seaweed *Gracilaria* spp. obtained at pH 3 against the bacteria S. *aureus* and *E. coli*. The diameter of inhibition using the disc diffusion method was 1.4 mm for S. *aureus* and 2 mm for *E. coli*. The sequence of the peptide fraction that provides activity is the read sequence, namely VVINADAK, TVTLEESGK, SIVNADAEAR, EVTSSLVTDAGK, SHNGSDEWK, SAAEQSAPE, GAEDGNVYDEK.

The longest fragment of EVTSSLVTDAGK is known to come from the allophycocyanin complex or pigment from *Gracilaria changii* with a pI value of 5.6. The predicted structure of the peptide is coil and sheet. The shortest fragment of VVINADAK is known to come from the Cpe complex or cytoplasm polyadenylation element from *Gracilaria changii* with a pI value of 5.31. Our model GP4.1 and GP4.2 model (VVINADAK) had high binding affinities with the energy score of -10,6 and -10,8 kcal/mol, with high hydrogen bond found as compared to the chloramphenicol interactions.

Acknowledgements

This study was financially supported by the Ministry of Education and Culture, Innovative and Research Council, Indonesia, Master Thesis Research Grant (No. 0536/E5/PG.02.00/2023).

Conflict of Interest

There is no conflict of interest in this article.

Authors Contibutions

Klara Kharisma Bunga Chandra conducted the research experiment and wrote the manuscript, Dr. Tri Rini Nuringtyas conducted the proteomic and antibacterial analysis, revised the manuscript, and Prof. Dr. Tri Joko Raharjo designed the research plan, wrote and revised the manuscript. All authors agreed to the final version of this manuscript.

References

Ajesh, K., & Sreejith, K. (2009). *Peptides Peptide antibiotics/ : An alternative and effective antimicrobial strategy to circumvent fungal infections*. *30*, 999–1006. https://doi.org/10.1016/j.peptides.2009.01.026

Alanis, A. J. (2005). Resistance to antibiotics: Are we in the post-antibiotic era? *Archives of Medical Research*, *36*(6), 697–705. https://doi.org/10.1016/j.arcmed.2005.06.009

Alsenani, F., Tupally, K. R., Chua, E. T., Eltanahy, E., Alsufyani, H., Parekh, H. S., & Schenk, P. M. (2020). Evaluation of microalgae and cyanobacteria as potential sources of antimicrobial compounds. *Saudi Pharmaceutical Journal*, *28*(12), 1834–1841. https://doi.org/10.1016/j.jsps.2020.11.010

Alvarez, C., Félix, C., & Lemos, M. F. L. (2023). The Antiviral Potential of Algal Lectins. *Marine Drugs*, *21*(10). https://doi.org/10.3390/md21100515

Aoki, J., Sasaki, D., & Asayama, M. (2021). *Development of a method for phycocyanin recovery from filamentous cyanobacteria and evaluation of its stability and antioxidant capacity*. 1–10.

Asayama, M. (2012). Overproduction and easy recovery of target gene products from cyanobacteria, photosynthesizing microorganisms. *Applied Microbiology and Biotechnology*, *95*(3), 683–695. https://doi.org/10.1007/s00253-012-3989-0

Bahar, A. A., & Ren, D. (2013). *Antimicrobial Peptides*. 1543–1575. https://doi.org/10.3390/ph6121543

Barre, A., Van Damme, E. J. M., Klonjkowski, B., Simplicien, M., Sudor, J., Benoist, H., & Rougé, P. (2022). Legume Lectins with Different Specificities as Potential Glycan Probes for Pathogenic Enveloped Viruses. *Cells*, *11*(3), 1–2. https://doi.org/10.3390/cells11030339

Beaulieu, L., Bondu, S., Doiron, K., Rioux, L. E., & Turgeon, S. L. (2015). Characterization of antibacterial activity from protein hydrolysates of the macroalga Saccharina longicruris and identification of peptides implied in bioactivity. *Journal of Functional Foods*, *17*, 685–697. https://doi.org/10.1016/j.jff.2015.06.026

Biswas, T., Houghton, J. L., Garneau-Tsodikova, S., & Tsodikov, O. V. (2012). The structural basis for substrate versatility of chloramphenicol acetyltransferase CATI. *Protein Science*, *21*(4), 520–530. https://doi.org/10.1002/pro.2036

Boob, S., Soun, P., Prithivraj, M., & G, V. (2010). *Biochemical Characterization of Protein Isolated from Seaweed , Gracilaria edulis*. *2*(1), 35–37.

Charlesworth, A., Meijer, H. A., & De Moor, C. H. (2013). Specificity factors in cytoplasmic polyadenylation. *Wiley*

Interdisciplinary Reviews: RNA, *4*(4), 437–461. https://doi.org/10.1002/wrna.1171

Chiara, M., John, C., Orla, H., & Joan, S. (2021). Using an Ensemble to Identify and Classify Macroalgae Antimicrobial Peptides. *Interdisciplinary Sciences: Computational Life Sciences*, *13*(2), 321–333. https://doi.org/10.1007/s12539-021-00435-6

Chuang, P., Tao, F., Qi, B., Xiang, H., Chen, S., & Yang, X. (2023). A novel antioxidant protein of non-phycobiliprotein family derived from marine red alga Porphyra haitanensis. *Journal of the Science of Food and Agriculture*, *103*(11), 5277–5287. https://doi.org/10.1002/jsfa.12601

Ciumac, D., Gong, H., Hu, X., & Lu, J. R. (2019). Membrane targeting cationic antimicrobial peptides. *Journal of Colloid and Interface Science*, *537*, 163–185. https://doi.org/10.1016/j.jcis.2018.10.103

Conde, E., Balboa, E. M., Parada, M., & Falqué, E. (2013). Algal proteins, peptides and amino acids. In *Functional Ingredients from Algae for Foods and Nutraceuticals*. https://doi.org/10.1533/9780857098689.1.135

Cotton, G. C., Lagesse, N. R., Parke, L. S., & Meledandri, C. J. (2019). Antibacterial nanoparticles. In *Comprehensive Nanoscience and Nanotechnology* (Vols. 1–5). Elsevier Ltd. https://doi.org/10.1016/B978-0-12-803581-8.10409-6

De Vries, S. J., Van Dijk, M., & Bonvin, A. M. J. J. (2010). The HADDOCK web server for data-driven biomolecular docking. *Nature Protocols*, *5*(5), 883–897. https://doi.org/10.1038/nprot.2010.32

Garcia-vaquero, M., Mora, L., & Hayes, M. (2019). *In Vitro and In Silico Approaches to Generating and Identifying Angiotensin-Converting Enzyme I Inhibitory Peptides from Green Macroalga*. 1–19. https://doi.org/10.3390/md17040204

Gogoladze, G., Grigolava, M., Vishnepolsky, B., Chubinidze, M., Duroux, P., Lefranc, M. P., & Pirtskhalava, M. (2014). DBAASP: Database of antimicrobial activity and structure of peptides. *FEMS Microbiology Letters*, *357*(1), 63–68. https://doi.org/10.1111/1574-6968.12489

Holanda, M. L., Pereira, M. G., & Biologia, D. (2005). *Differential activity of a lectin from Solieria filiformis against human pathogenic bacteria*. *38*, 1769–1773.

Huan, Y., Kong, Q., Mou, H., & Yi, H. (2020). Antimicrobial Peptides: Classification, Design, Application and Research Progress in Multiple Fields. *Frontiers in Microbiology*, *11*(October), 1–21. https://doi.org/10.3389/fmicb.2020.582779

Hwang, H. J., Han, J. W., Jeon, H., Cho, K., Kim, J. H., Lee, D. S., & Han, J. W. (2020). Characterization of a novel mannose-binding lectin with antiviral activities from red alga, grateloupia chiangii. *Biomolecules*, *10*(2). https://doi.org/10.3390/biom10020333

Iolovitch, M. (2020). Chapter 19. *On a Clear April Morning*, 64–69. https://doi.org/10.1515/9781644692998-022

Ivshina, M., Lasko, P., & Richter, J. D. (2014). Cytoplasmic polyadenylation element binding proteins in development, health, and disease. *Annual Review of Cell and Developmental Biology*, *30*, 393–415. https://doi.org/10.1146/annurev-cellbio-101011-155831

Jose, A., Bunster, M., & Vorphal, A. (2017). *Structural models of the different trimers present in the core of phycobilisomes from Gracilaria chilensis based on crystal structures and sequences ´ a*. 1–15.

Kawasaki, S., Yamazaki, K., Nishikata, T., Ishige, T., Toyoshima, H., & Miyata, A. (2020). Photooxidative stress-inducible orange and pink water-soluble astaxanthin-binding proteins in eukaryotic microalga. *Communications Biology*, *3*(1), 1–9. https://doi.org/10.1038/s42003-020-01206-7

Kowalska-Krochmal, B., & Dudek-Wicher, R. (2021). The minimum inhibitory concentration of antibiotics: Methods, interpretation, clinical relevance. *Pathogens*, *10*(2), 1–21. https://doi.org/10.3390/pathogens10020165

Lei, J., Sun, L. C., Huang, S., Zhu, C., Li, P., He, J., Mackey, V., Coy, D. H., & He, Q. Y. (2019). The antimicrobial peptides and their potential clinical applications. *American Journal of Translational Research*, *11*(7), 3919–3931.

Li, S., Wang, Y., Xue, Z., Jia, Y., Li, R., He, C., & Chen, H. (2021). The structure-mechanism relationship and mode of actions of antimicrobial peptides: A review. *Trends in Food Science and Technology*, *109*(January), 103–115. https://doi.org/10.1016/j.tifs.2021.01.005

Maliki, I. M., Misson, M., Teoh, P. L., Rodrigues, K. F., & Yong, W. T. L. (2022). Production of Lectins from Marine Algae: Current Status, Challenges, and Opportunities for Non-Destructive Extraction. *Marine Drugs*, *20*(2). https://doi.org/10.3390/md20020102

Mishra, A. K. (2018). *Sargassum , Gracilaria and Ulva Exhibit Positive Antimicrobial Activity against Human Pathogens*. *5*, 1–12. https://doi.org/10.4236/oalib.1104258

Mukherjee, C., Suryawanshi, P. G., Kalita, M. C., Deka, D., Aranda, D. A. G., & Goud, V. V. (2022). Polarity-wise successive solvent extraction of Scenedesmus obliquus biomass and characterization of the crude extracts for broad-spectrum antibacterial activity. *Biomass Conversion and Biorefinery*, *0123456789*. https://doi.org/10.1007/s13399-022-02432-1

Naik, S., & Kumar, S. (2022). Lectins from plants and algae act as anti viral against HIV , influenza and coronaviruses. *Molecular Biology Reports*, *49*(12), 12239–12246. https://doi.org/10.1007/s11033-022-07854-8

Nasri, M. (2017). *Chapter Four - Protein Hydrolysates and Biopeptides: Production, Biological Activities, and Applications in Foods and Health Benefits. A Review* (F. Toldrá (ed.); Vol. 81, pp. 109–159). Academic Press. https://doi.org/https://doi.org/10.1016/bs.afnr.2016.10.003

Niu, L., Zhang, H., Wu, Z., Wang, Y., Liu, H., Wu, X., & Wang, W. (2018). Modified TCA/acetone precipitation of plant proteins for proteomic analysis. *PLoS ONE*, *13*(12), 1–13. https://doi.org/10.1371/journal.pone.0202238

Olsen, J. V., Ong, S. E., & Mann, M. (2004). Trypsin cleaves exclusively C-terminal to arginine and lysine residues. *Molecular and Cellular Proteomics*, *3*(6), 608–614. https://doi.org/10.1074/mcp.T400003-MCP200

Pajot, A., Lavaud, J., Carrier, G., Garnier, M., Saint-Jean, B., Rabilloud, N., Baroukh, C., Bérard, J. B., Bernard, O., Marchal, L., & Nicolau, E. (2022). The Fucoxanthin Chlorophyll a/c-Binding Protein in Tisochrysis lutea: Influence of Nitrogen and Light on Fucoxanthin and Chlorophyll a/c-Binding Protein Gene Expression and Fucoxanthin Synthesis. *Frontiers in Plant Science*,

13(February), 1–17. https://doi.org/10.3389/fpls.2022.830069

Pettigrew, D., Anderson, K. L., Billington, J., Cota, E., Simpson, P., Urvil, P., Rabuzin, F., Roversi, P., Nowicki, B., Du Merle, L., Bouguénec, C. Le, Matthews, S., & Lea, S. M. (2004). High resolution studies of the Afa/Dr adhesin DraE and its interaction with chloramphenicol. *Journal of Biological Chemistry*, *279*(45), 46851–46857. https://doi.org/10.1074/jbc.M409284200

Proteins, B., Acids, A., & Macroalgae, F. (2011). *Bioactive proteins, peptides, and amino acids from macroalgae 1*. *232*, 218–232. https://doi.org/10.1111/j.1529-8817.2011.00969.x

Raharjo, T. J., Utami, W. M., Fajr, A., Haryadi, W., & Swasono, R. T. (2021). *Antibacterial Peptides from Tryptic Hydrolysate of Ricinus communis Seed Protein Fractionated Using Cation Exchange Chromatography*. *32*(1), 74–85.

Salwiczek, M., Nyakatura, E. K., Gerling, U. I. M., Ye, S., & Koksch, B. (2012). Fluorinated amino acids: Compatibility with native protein structures and effects on protein–protein interactions. *Chemical Society Reviews*, *41*(6), 2135–2171. https://doi.org/10.1039/c1cs15241f

Skoèibušiæ, M., Laciæ, S., & Rašiæ, Z. (2019). Evaluation of Antimicrobial Potential of the Marine Cyanobacterium, Rivularia mesenterica. In *Journal of Advances in Microbiology* (pp. 1–11). https://doi.org/10.9734/jamb/2019/v16i430128

Steen, H., & Mann, M. (2004). The ABC's (and XYZ's) of peptide sequencing. *Nature Reviews Molecular Cell Biology*, *5*(9), 699–711. https://doi.org/10.1038/nrm1468

Sun, K. L., Gao, M., Wang, Y. Z., Li, X. R., Wang, P., & Wang, B. (2022). Antioxidant Peptides From Protein Hydrolysate of Marine Red Algae Eucheuma cottonii: Preparation, Identification, and Cytoprotective Mechanisms on H2O2 Oxidative Damaged HUVECs. *Frontiers in Microbiology*, *13*(April), 1–14. https://doi.org/10.3389/fmicb.2022.791248

Teixeira, E. H., Napimoga, M. H., Carneiro, V. A., De Oliveira, T. M., Nascimento, K. S., Nagano, C. S., Souza, J. B., Havt, A., Pinto, V. P. T., Gonçalves, R. B., Farias, W. R. L., Saker-Sampaio, S., Sampaio, A. H., & Cavada, B. S. (2007). In vitro inhibition of oral streptococci binding to the acquired pellicle by algal lectins. *Journal of Applied Microbiology*, *103*(4), 1001–1006. https://doi.org/10.1111/j.1365-2672.2007.03326.x

Tu, M., Feng, L., Wang, Z., Qiao, M., Shahidi, F., Lu, W., & Du, M. (2017). Sequence analysis and molecular docking of antithrombotic peptides from casein hydrolysate by trypsin digestion. *Journal of Functional Foods*, *32*, 313–323. https://doi.org/10.1016/j.jff.2017.03.015

Wang, Y., Yang, Y., Chen, Y., & Zhao, H. (2016). Computer-aided design , structural dynamics analysis , and in vitro susceptibility test of antibacterial peptides incorporating unnatural amino acids against microbial infections. *Computer Methods and Programs in Biomedicine*, *134*, 215–223. https://doi.org/10.1016/j.cmpb.2016.06.005

Xiang, H., Cao, F., Ming, D., Zheng, Y., Dong, X., Zhong, X., Mu, D., Li, B., Zhong, L., Cao, J., Wang, L., Ma, H., Wang, T., & Wang, D. (2017). *Aloe-emodin inhibits Staphylococcus aureus biofilms and extracellular protein production at the initial adhesion stage of biofilm development*. https://doi.org/10.1007/s00253-017-8403-5

Yu, B., Zhang, Y., Yang, L., Xu, J., & Bu, S. (2021). Analysis of antibiotic resistance phenotypes and genes of escherichia coli from healthy swine in guizhou, china. *Onderstepoort Journal of Veterinary Research*, *88*(1), 1–8. https://doi.org/10.4102/OJVR.V88I1.1880